# Neutron scattering study of the ferromagnetic superconductor $UGe_2$

N. Kernavanois, B. Grenier,* A. Huxley, E. Ressouche, J. P. Sanchez, and J. Flouquet
*Département de Recherche Fondamentale sur la Matière Condensée, SPSMS, CEA/Grenoble, 17 rue des Martyrs, 38054 Grenoble Cédex 9, France*

(Received 3 March 2001; published 11 October 2001)

Unpolarized and polarized neutron scattering experiments have been performed at ambient pressure on a single crystal of the itinerant electron superconductor $UGe_2$ in both the ferromagnetic and the paramagnetic phases. Unpolarized neutrons have confirmed the $ZrGa_2$-type orthorhombic crystal structure of $UGe_2$ and a ferromagnetic ordering below $T_C=53$ K with the moments aligned along the *a* axis. No evidence of any modulated component for the magnetic structure has been found. Polarized neutron data have shown a large and almost spherical magnetization distribution at the U sites and no induced moment at the Ge sites. Refinements of the magnetic structure factors within the dipolar approximation allow the magnitude of the orbital and spin uranium moments to be quantified, and a comparison to the measured static magnetization reveals that there is no diffuse contribution.

DOI: 10.1103/PhysRevB.64.174509 PACS number(s): 74.70.Tx, 61.12.−q, 31.70.−f

## I. INTRODUCTION

The first studies on $UGe_2$ were realized in the late fifties. Makarov *et al.*[1] reported that this compound crystallizes in an orthorhombic structure of the $ZrSi_2$ type (space group *Cmcm*) but the fit to this structure had a poor reliability factor (25%). One year later, the study performed by Olsen *et al.*[2] was more in favor of an orthorhombic structure derived from a distorted structure of the $ThSi_2$ type (space group $Amm2$), despite the fact that no reliability factor was given. Susceptibility measurements realized by the same group on a powder sample showed a ferromagnetic ordering at a Curie temperature $T_C=52$ K with a magnetic moment at saturation of $0.8\mu_B$/f.u.[2]

Nearly 25 years later, Menovsky *et al.*[3] reported on the first susceptibility and magnetization experiments on single crystals. These measurements confirmed the ferromagnetic behavior of $UGe_2$ and the value of the Curie temperature (52 K). The magnetization turned out to be strongly anisotropic with an easy magnetization axis corresponding to the *c* axis in the $ZrSi_2$ orthorhombic structure suggested by Makarov *et al.*[1] The value of the easy axis magnetization at saturation was $1.43\mu_B$/f.u., that is considerably larger than the one found on the polycrystal by Olsen *et al.*[2] ($0.8\mu_B$/f.u.) owing to the strong anisotropy.

Then, it was solely in the nineties that $UGe_2$ renewed interest. Several new experimental studies were realized.[4–9] Among them, specific heat measurements[5] led to a Sommerfeld coefficient $\gamma$ of 35 $\mathrm{mJ\,K^{-2}\,mol^{-1}}$. This relatively large value indicates that $UGe_2$ has a moderate heavy-fermion behavior. Band structure calculations[10] (performed within the assumed $ZrSi_2$ structure type), together with de Haas–van Alphen experiments[11] gave evidence for an itinerant ferromagnetic behavior. Measurements of the thermal expansion coefficients under an applied pressure[12] indicated the existence of a magnetovolumic effect at $T_C$, the decrease of the Curie temperature with pressure, and the disappearance of the magnetic order at 20 kbar. Due to this increasing interest, a better knowledge of the crystallographic structure was necessary and led Oikawa *et al.*[13] and Boulet *et al.*[14] to independently reinvestigate it. They determined that $UGe_2$ actually crystallizes in the orthorhombic $ZrGa_2$ structure type (space group *Cmmm*) with a reliability factor of ~5%, instead of the $ZrSi_2$ structure reported by Makarov *et al.*[1] In this $ZrGa_2$ structure, the room temperature crystallographic cell is described by $a=3.97$ Å, $b=15.1$ Å, and $c=4.11$ Å, the easy magnetization axis being the shorter one that is *a*.

Recently, Saxena *et al.*[15] announced the appearance of a nonconventional superconductivity induced by pressure in $UGe_2$ single crystals. Combining susceptibility and resistivity measurements together with neutron scattering experiments, Saxena *et al.*[15] and Huxley *et al.*[16] have determined the full pressure-temperature phase diagram of $UGe_2$. The superconductivity appears at pressures higher than 10 kbar, and even more striking is the fact that the highest superconductive transition temperature ($T_{sc}=0.8$ K at ~12 kbar) corresponds to a Curie temperature almost 45 times larger than $T_{sc}$. Moreover, the disappearance of the superconductivity at ~16 kbar occurs with the disappearance of the ferromagnetic order. This feature suggests that superconductivity and ferromagnetic ordering are cooperative effects.

Whether ferromagnetic fluctuations are the origin of pairing is not yet determined, but the large polarization of electron bands leads to suspect a triplet superconducting pairing. Models based on ferromagnetic spin fluctuations predict that superconductivity may occur on both sides of the critical pressure $P_C$ for the suppression of the ferromagnetism.[17,18] In $UGe_2$, the situation is different since superconductivity is only found on the ferromagnetic side. This could be explained by a change in the magnetic transition from second order to first order at a pressure below the critical pressure, as has been suggested from susceptibility measurements under pressure.[16] However ferromagnetic fluctuations may not be the only driving mechanism which governs the appearance of superconductivity under pressure. Resistivity measurements have also evidenced an additional transition within the ferromagnetic state. The characteristic temperature of this transition $T_X$, decreases with pressure and disappears at a pressure close to the one where superconductivity

 

is the strongest.[16] This transition is quite similar to that observed in $\alpha$ uranium, a material that structurally resembles $UGe_2$. For $\alpha$ uranium, there is direct evidence that the anomalies are due to the formation of a charge density wave (CDW), resulting from a nesting at the Fermi surface. For $UGe_2$, band structure calculations also suggest that there is a possible proximity to nesting, with the apparition of a similar CDW. This supposed CDW would result in an associated spin density wave, and therefore a modulation of the ferromagnetic structure resulting in incommensurate Bragg peaks. However, different calculations[19,20] predict different nesting directions, and therefore these extra peaks, if they exist, are not obvious to find experimentally.

In this paper, we investigated in more details the magnetic structure of $UGe_2$ at ambient pressure, where the extrapolated $T_X$ value is close to 30 K. We therefore tested whether a significant modulation of the magnetic structure occurs even at a pressure $P=0$. If such a modulation exists, it is, however, expected to be very weak since it has not been detected by powder neutron scattering measurements.[13,14] Our study has been realized by the diffraction of unpolarized neutrons. In addition, using the polarized neutron scattering technique, we decided to investigate $5f$ orbital and spin contributions in order to determine more exactly the nature of the electronic magnetism.

The paper is divided into four parts. The next section is dedicated to the low-temperature nuclear structure refinement needed for both the magnetic structure study which is described in Sec. III and the polarized neutron measurements depicted in Sec. IV. These latter measurements have been performed both in the ferromagnetic ($T=6$ K) and the paramagnetic ($T=60$ K) phases. Conclusions are drawn in Sec. V.

All the experiments have been carried out on the same single crystal prepared by the Czochralski technique under a purified argon atmosphere. Further details on the sample preparation can be found in Ref. 16. The sample had a cylindrical shape ($\sim 1.9$ mm in height and $\sim 1.5$ mm in diameter) with the $a$ easy magnetization axis parallel to the cylinder axis.

The magnetic moment at saturation ($\mu^{\mathrm{sat}}$) of this sample has been determined with a SQUID magnetometer: it reaches $1.50(2)\mu_B$/f.u. Moreover it has been checked that under pressure, this sample has a behavior consistent with the published phase diagram.[15,16]

## II. NUCLEAR STRUCTURE REFINEMENT

The nuclear structure refinement has been realized on the D15-CEA-CRG (Collaborating Research Group) instrument of the ILL (Institut Laue-Langevin, Grenoble, France) in a four-circle geometry. In order to characterize precisely the extinction of the sample, two sets of data at 60 K (in the paramagnetic phase) were collected at two different wavelengths $\lambda=1.174$ and 0.854 Å. 416 and 355 reflections were measured respectively, corresponding to 154 and 136 independent reflections. Experimental data have been corrected for absorption (linear absorption coefficient, $\mu=0.0048$ mm$^{-1}$). A $\lambda/2$ correction has also been applied to the data set measured at $\lambda=1.174$ Å. The refined $\lambda/2$ contamination is 0.17(2)%.

This experiment confirmed the $ZrGa_2$ type structure reported in Refs. 13,14. The cell parameters values $a=3.997(3)$ Å, $b=15.039(7)$ Å, and $c=4.087(2)$ Å were found at 60 K. Structural parameters were refined using the program MXD,[21] combining the two experimental data sets obtained at the two wavelengths. The nuclear scattering lengths used were $0.84170\times10^{-12}$ cm and $0.81850\times10^{-12}$ cm for uranium and germanium atoms, respectively. The refinement led to a crystallographic weighted residual factor $R_\omega(F^2)=5.25\%$ (Ref. 22). This refinement included a Becker-Coppens Lorentzian correction of the extinction.[23] This correction turned out to be rather weak (less than 10% of the most concerned reflections) and led to an extinction coefficient $g$ of 148(22) rad$^{-1}$ corresponding to a crystal mosaicity $\eta=6.55(97)'$ [$\eta=1/(2\sqrt{\pi g})$]. Results are presented in Table I and Fig. 1 shows a view of the $UGe_2$ crystallographic cell with the thermal motion ellipsoids at 60 K.

## III. MAGNETIC STRUCTURE STUDY

Two data sets, at 5 and 30 K, have been collected on the D23-CEA-CRG instrument of the ILL at a wavelength $\lambda=1.285$ Å. 108 reflections have been measured at each temperature. The refinements performed are in good agreement with a ferromagnetic structure, with the uranium moments pointing along the easy magnetization axis $a$ [$\chi^2=2.05$ and 1.46; $R_\omega(F^2)=11.72\%$ and 11.45% for data obtained at 5 and 30 K, respectively]. The magnetic moment on the uranium sites are $\mu^U=1.48(2)\mu_B$ at 5 K and $1.29(2)\mu_B$ at 30 K.

We have also measured the temperature dependence of the integrated intensity of the magnetic reflection (0 0 1). The result is presented in Fig. 2.

Between $0.90\times T_C$ and $T_C$, the integrated intensity fits a law $(1-T/T_C)^{2\beta}$ corresponding to a magnetization variation $M(T)\propto(1-T/T_C)^{\beta}$, with $T_C=53$ K (Fig. 2). The refined value of the critical exponent $\beta$ of 0.36(1) is in good agreement with the 3D nature of this system.[24]

In order to shed light on a possible modulation of the magnetic structure, we have first realized a refinement of the (0 0 1) Bragg reflection with a Gaussian indicating that its full width at half maximum (FWHM) does not change significantly with the temperature [FWHM$\sim$0.032(1) r.l.u.]. We have then performed several $Q$ scans along the high symmetry axes $a^\star$, $b^\star$, and $c^\star$, of the reciprocal space in the ordered (at $T=5$ K) and paramagnetic (at $T=60$ K) phases. The differences performed between the higher and lower temperature associated scans indicate a zero magnetic contribution for noninteger $Q$ value whatever the considered direction. One of these scans and the associated difference are presented in Fig. 3. They correspond to measurements realized along the $c^\star$ axis.

Thus, our measurements confirmed neither the nesting at around $Q\sim(0.45\times2\pi/a,0,0)$ indicated by LDA+U approach,[19], nor the nesting instability predicted along the

TABLE I. Atomic positions and thermal anisotropic factors $U_{ii}$ in $UGe_2$ (space group *Cmmm*). The Debye-Waller factor is defined as $\exp\{-2\pi^2[(h^2/a^2)U_{11}+(k^2/b^2)U_{22}+(l^2/c^2)U_{33}]\}$ and $B_{equi}=(8\pi^2/3)(U_{11}+U_{22}+U_{33})$. These values are deduced from the neutron scattering measurements realized at 60 K.

| Atoms | Site | Positions | $U_{ii}$ (Å$^2$) | $B_{equi}$ (Å$^2$) |
|---|---|---|---|---|
| U | 4*j* | $(0,y_U,\frac{1}{2})$ $y_U=0.14094(3)$ | $U_{11}=0.00101(23)$ $U_{22}=0.00116(23)$ $U_{33}=0.00244(24)$ | $B_U=0.12(3)$ |
| $Ge_1$ | 4*i* | $(0,y_{Ge^1},0)$ $y_{Ge^1}=0.30779(4)$ | $U_{11}=0.00095(25)$ $U_{22}=0.00483(26)$ $U_{33}=0.00240(27)$ | $B_{Ge_1}=0.22(3)$ |
| $Ge_2$ | 2*a* | (0,0,0) | $U_{11}=0.00185(33)$ $U_{22}=0.00155(32)$ $U_{33}=0.00241(33)$ | $B_{Ge_2}=0.15(4)$ |
| $Ge_3$ | 2*c* | $(\frac{1}{2},0,\frac{1}{2})$ | $U_{11}=0.00029(34)$ $U_{22}=0.00290(33)$ $U_{33}=0.00518(36)$ | $B_{Ge_3}=0.22(4)$ |

*c*-axis direction by another relativistic augmented plane wave calculation.[20]

All these features confirm the ferromagnetic order in $UGe_2$. Nevertheless, taking into account both the background amplitude and the magnetic contribution to the (0 0 1) reflection, one can reasonably estimate that if an antiferromagnetic contribution occurs at a propagation vector situated along the studied directions, it would be less than $0.06\mu_B$.

## IV. DETERMINATION OF THE MAGNETIZATION DISTRIBUTION BY POLARIZED NEUTRON DIFFRACTION

The classical polarized beam method consists in measuring the ratio, called the flipping ratio, between the intensities $I^+$ and $I^-$ of a Bragg reflection, for an incident polarization of the neutron beam respectively parallel (+) and antiparallel (−) to the applied field direction. This technique takes advantage of an interference term in the cross sections between the magnetic and nuclear signals (provided that they occur at the same point of the reciprocal space). It is well adapted to the study of ferromagnetic, ferrimagnetic and paramagnetic systems and its sensitivity to small magnetic contributions is much larger than the conventional unpolarized beam method. Details of this technique can be found in Ref. 25.

The flipping ratio measurements have been carried out on the D23-CEA-CRG diffractometer of the ILL with a wavelength $\lambda=1.285$ Å provided by an Heusler alloy monochromator [polarization rate of the incident beam $p=-0.9560(5)$; flipping efficiency $e=0.981(4)$]. Two series of measurements at respectively 6 K (ferromagnetic phase)

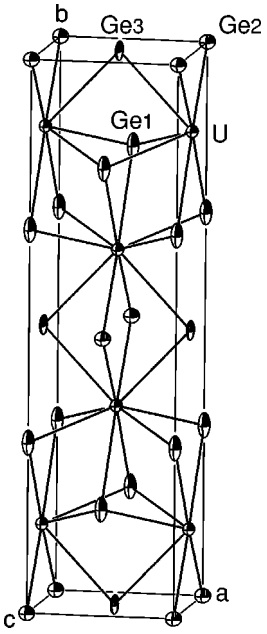


FIG. 1. View of the $UGe_2$ structure with thermal ellipsoids at 60 K.

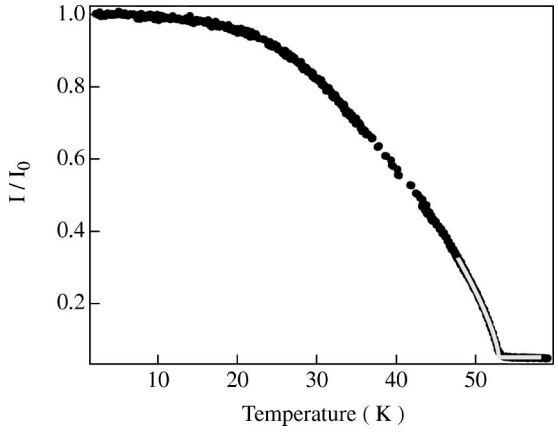


FIG. 2. Temperature dependence of the normalized integrated intensity of the magnetic reflection (0 0 1). Experimental points are drawn as full black circles. Refinement using a $(1-T/T_C)^{2\beta}$ law between $0.90\times T_C$ and $T_C$, with $\beta=0.36(1)$ and $T_C=53$ K, is presented in solid gray line.

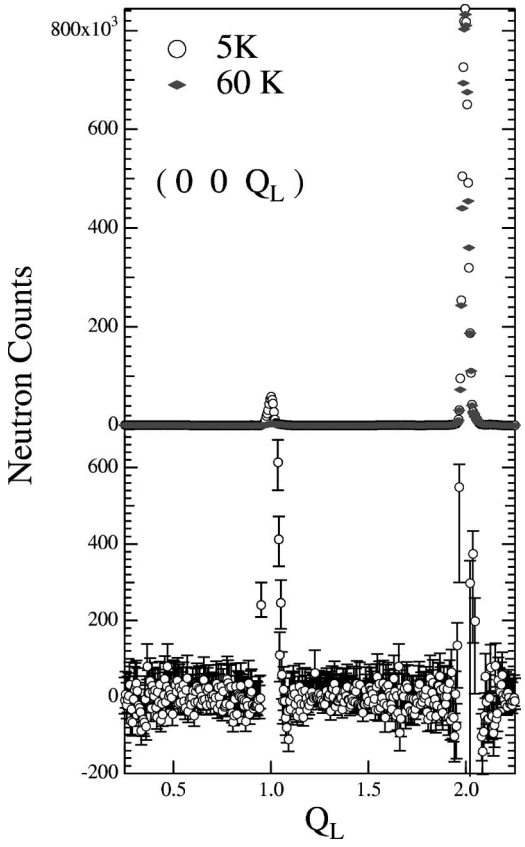


FIG. 3. Upper panel: (0 0 $Q_L$) scans realized at 5 and 60 K. Lower panel: Difference of the associated *Q* scans realized at 5 and 60 K. The peaks at (0 0 1) and (0 0 2) are due to the known ferromagnetic structure. No additional peaks are seen.

and 60 K (paramagnetic phase) have been performed under a magnetic field $B_{ext}=4.6$ T applied along the easy magnetization axis *a*. 116 and 120 flipping ratios have been collected at 6 and 60 K, leading to 38 and 40 independent magnetic structure factors $F_M(h\,k\,l)$ up to $\sin\theta/\lambda=0.5$ Å$^{-1}$.

The $F_M(h\,k\,l)$ are the Fourier components of the magnetization distribution. To recover this distribution, one has to solve the inverse Fourier problem for which several methods can be used:

### A. Fourier analysis using the three-dimensional maximum entropy (MaxEnt) technique

This technique gives the most probable magnetization distribution map compatible with the measured structure factors and their experimental uncertainties.[26–28] It is much more powerful than the classical Fourier synthesis since it does not make any assumption concerning the unmeasured Fourier components and it takes into account the experimental uncertainties.

The magnetization distributions deduced from data sets measured in the paramagnetic and ferromagnetic phases were found to be equivalent (with a different overall amplitude). Figure 4 shows the projections of this magnetization distribution at 6 K along the three crystallographic axes *a*, *b*, and *c*. These maps have been obtained using a flat starting

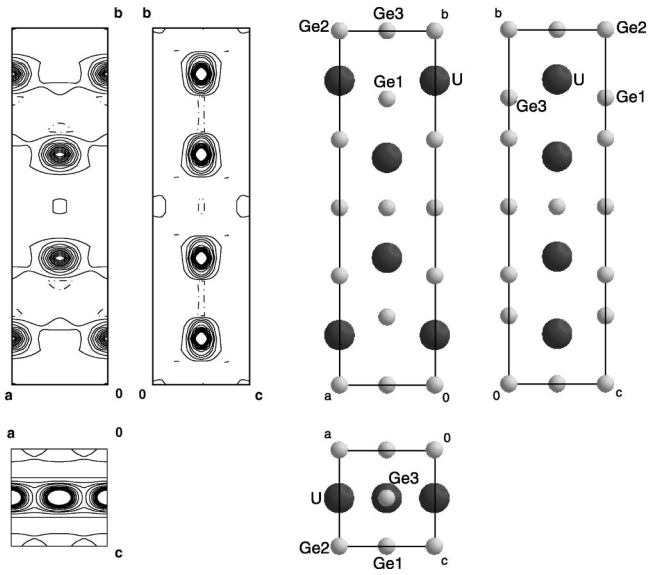


FIG. 4. Projections of the magnetization distribution and of the unit cell of $UGe_2$ along the crystallographic axis *c*, *a*, and *b*. Positive contour lines, drawn as full lines, correspond to values from 0.05 to $0.35\mu_B$ Å$^{-2}$ with a step of $0.10\mu_B$ Å$^{-2}$ and from 0.35 to $1.85\mu_B$ Å$^{-2}$ with a step of $0.20\mu_B$ Å$^{-2}$. The negative contour line (dashed line) corresponds to $-0.05\mu_B$ Å$^{-2}$.

hypothesis[29] and taking into account the magnetization value that corresponds to $F_M(0\,0\,0)=4\times\mu^{sat}=6.00(8)\mu_B$ (since we have four formula units in the crystallographic cell).

We can conclude from these maps that the magnetization is essentially localized on the uranium sites. No sizeable magnetic contribution is detected on the germanium sites. A small negative contour line is present on these maps. It could be ascribed to spurious oscillations of the magnetization distribution due to the finite number of reflections used for the reconstruction. Similarly, the first positive contour line can be also ascribed to these truncation effects and gives a quantitative idea of the uncertainties in the reconstructions.

### B. Model refinement

In order to quantify the magnetic contributions observed with the MaxEnt technique, we have realized a least-squares refinement of the magnetic structure factors, using the Cambridge Crystallography Subroutine Library.[30]

This refinement was done within the dipolar approximation.[31] In this approximation, the uranium form factor can be written as $f^U(h\,k\,l)=\langle j_0\rangle^U+C_2\ \langle j_2\rangle^U$ with $\langle j_0\rangle^U$ and $\langle j_2\rangle^U$ the radial integrals, for a uranium ion with either the configuration $3+$ or $4+$, tabulated in Ref. 32. $C_2=\mu_L^U/\mu^U$ is the ratio between the orbital and total uranium magnetic moments. We have also tried to refine a contribution on the germanium sites assuming a 3*d* form factor $\langle j_0\rangle^{Ge}$ (Ref. 33). The choice of a Ge-3*d* form factor instead of a Ge-4*p* one is justified by the sharp decrease as a function of $\sin\theta/\lambda$ of the 4*p* electron form factor (Fig. 5). Indeed, the Ge-4*p* form factor is very localized in reciprocal space implying a diffuse 4*p* magnetic contribution in direct space.

At 6 and 60 K, no sizeable magnetic contributions on the germanium sites have been found. At 6 K, $\mu^{Ge_1}$

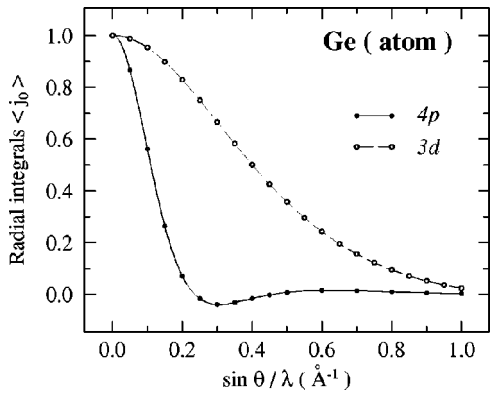


FIG. 5. Radial integrals $\langle j_0 \rangle$ of the electronic shells $4p$ and $3d$ of the germanium atom (configuration: [Ar] $3d^{10}\ 4s^2\ 4p^2$) (Ref. 33).

$=-0.004(10)\mu_B/\mathrm{Ge}_1$, $\mu^{\mathrm{Ge}_2}=0.018(13)\mu_B/\mathrm{Ge}_2$, $\mu^{\mathrm{Ge}_3}=-0.009(15)\mu_B/\mathrm{Ge}_3$, in agreement with the result obtained with the MaxEnt technique. We have therefore fixed the Ge contributions to zero and the final refinements are presented in Table II. In this table, the total magnetizations $\mu^{\mathrm{bulk}}$ at 6 and 60 K are indicated. These values have been determined by magnetization measurements with a SQUID magnetometer. We point out that at 6 K, $\mu^{\mathrm{bulk}}$ reaches the magnetization value at saturation $\mu^{\mathrm{sat}}=1.50(2)\mu_B/\mathrm{f.u.}$ Polarized neutron scattering results are also indicated: for both temperatures and U configurations, the refined values of the uranium magnetic moment $\mu^{\mathrm{U}}$ and of the orbital uranium moment $\mu_{\mathrm{L}}^{\mathrm{U}}$ are given. From these results, we can deduce the values of $C_2=\mu_{\mathrm{L}}^{\mathrm{U}}/\mu^{\mathrm{U}}$ and $\mathrm{R_L}=C_2/(C_2-1)=-\mu_{\mathrm{L}}^{\mathrm{U}}/\mu_{\mathrm{S}}^{\mathrm{U}}$ together with the diffuse magnetic contribution $\mu^{\mathrm{cond}}=\mu^{\mathrm{bulk}}-\mu^{\mathrm{U}}$. $C_2$ and $\mathrm{R_L}$ experimental values should be compared to the free-ion values $\mathrm{C_2^{IC}}$ and $\mathrm{R_L^{IC}}$ calculated within the intermediate coupling (IC) scheme.[34]

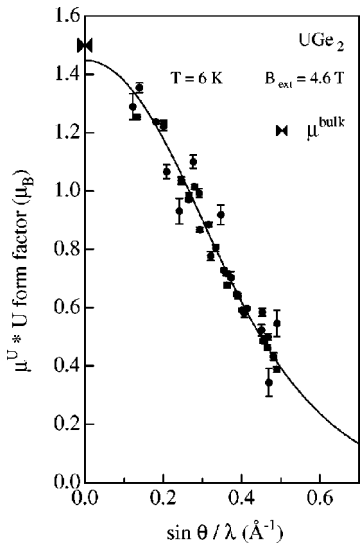


FIG. 6. Uranium form factor multiplied by $\mu^{\mathrm{U}}$, as a function of $\sin\theta/\lambda$. Measurements have been performed on $UGe_2$ at 6 K and 4.6 T. Points correspond to experimental data. The fit, assuming a $U^{3+}$ configuration, is drawn with a full line. The magnetic moment $\mu^{\mathrm{bulk}}$ which reaches its saturation value ($\mu^{\mathrm{sat}}$) is also indicated.

Figures 6 and 7 present the uranium form factors (multiplied by the U magnetic moment values) observed at 6 and 60 K, respectively, together with the associated calculated ones assuming a $U^{3+}$ configuration. Due to the minor differences between the form factors of $U^{3+}$ and $U^{4+}$, the refinements performed for these two states are completely equivalent and do not allow a determination of the uranium valency.

The U-$5f$ orbital to spin moments ratios for both $3+$ and $4+$ configurations are systematically reduced compared to the free-ion values (Ref. 34). It has been shown in previous

TABLE II. Summary of the different results obtained from magnetization and polarized neutron scattering measurements in $UGe_2$ at 6 and 60 K with an applied magnetic field of 4.6 T along *a*. The magnetic moment values are expressed in $\mu_B$/f.u. Theoretical free-ion values calculated in the intermediate coupling scheme are taken from Ref. 34.

| | $T=6$ K | | $T=60$ K | |
|---|---|---|---|---|
| $UGe_2$ | $U^{4+}$ | $U^{3+}$ | $U^{4+}$ | $U^{3+}$ |
| Magnetization measurements | | | | |
| $\mu^{\mathrm{bulk}}$ | 1.50(2) | | 0.79(2) | |
| Neutron experiments | | | | |
| $\mu^{\mathrm{U}}$ | 1.46(2) | 1.45(2) | 0.79(4) | 0.79(4) |
| $\mu_{\mathrm{L}}^{\mathrm{U}}$ | 2.37(4) | 2.62(4) | 1.22(7) | 1.35(7) |
| Deduced values | | | | |
| $C_2$ | 1.62(3) | 1.81(4) | 1.54(12) | 1.71(12) |
| $\mathrm{R_L}=-\mu_{\mathrm{L}}^{\mathrm{U}}/\mu_{\mathrm{S}}^{\mathrm{U}}$ | 2.60(15) | 2.24(10) | 2.84(55) | 2.41(37) |
| $\mu^{\mathrm{cond}}=\mu^{\mathrm{bulk}}-\mu^{\mathrm{U}}$ | 0.04(3) | 0.05(3) | 0.00(5) | 0.00(5) |
| Free-ion values | $U^{4+}$ ($5f^2$) | $U^{3+}$ ($5f^3$) | | |
| $\mathrm{C_2^{IC}}$ | 1.42 | 1.63 | | |
| $\mathrm{R_L^{IC}}$ | 3.36 | 2.60 | | |

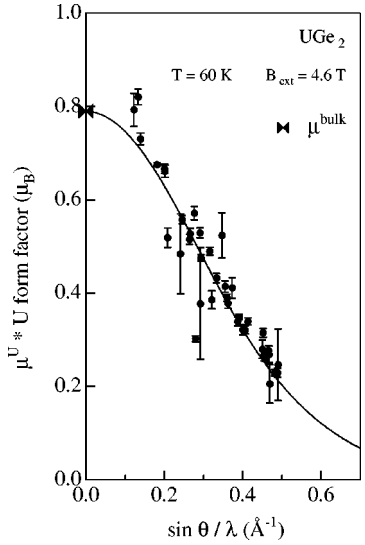


FIG. 7. Uranium form factor multiplied by $\mu^{U}$, as a function of $\sin\theta/\lambda$. Measurements have been performed on $UGe_2$ at 60 K and 4.6 T. Points correspond to experimental data. The fit, assuming a $U^{3+}$ configuration, is drawn with a full line.

polarized neutron scattering studies, that the delocalization of $5f$ electrons induces a drop of the $R_L$ ratio compared to the free-ion values (Ref. 35). Our result is thus in agreement with the itinerant ferromagnetism behavior concluded either from band structure calculations or from previous experiments.

Moreover, we notice a rather good agreement between our experimental U-$5f$ orbital to spin moments ratio of 2.24(10) assuming a $U^{3+}$ configuration and the one of 1.96 calculated by Shick *et al.*[19] with a U-$5f$ state occupation number of 2.81, i.e., close to a $3+$ valence state.

Between 6 and 60 K, $R_L$ values remain unchanged within the error bars (the measurements carried out in the paramagnetic phase has a larger uncertainty due to the smaller magnetic signal). No changes in the nature of the $5f$ wave functions are thus detected between the ferromagnetic and paramagnetic states.

The difference between the uranium magnetic contribution deduced from these measurements and the total magnetization is very weak whatever the temperature and the U configuration [$\sim 0.05(3)\mu_B$ at 6 K and $\sim 0.01(5)\mu_B$ at 60 K]. No sizeable diffuse contribution ($\mu^{cond}$) is thus observed.

## V. CONCLUSIONS

We have presented unpolarized and polarized neutron scattering measurements performed on a single crystal of $UGe_2$ in both the paramagnetic and ferromagnetic states. The unpolarized neutron scattering study has confirmed the nuclear and magnetic structures already determined on powder. The different scans we have performed in the reciprocal space do not indicate the presence of any additional peaks that could be a signature of a modulated phase. If such a modulation exists, its amplitude is less than $0.06\mu_B$/f.u. The polarized neutron scattering measurements allowed the determination of the $5f$ electron orbital and spin contributions in the paramagnetic and ferromagnetic phases. The $5f$ wave function nature does not seem to change between the phases. The ratios $R_L$ between orbital and spin moment values, are sytematically lower than the free-ion $U^{3+}$ or $U^{4+}$ values, whatever the phase. This feature is the signature of the hybridization of $5f$ electrons, despite the fact that neither a magnetic contribution localized on the Ge sites, nor a diffuse magnetic contribution have been detected. We point out that this situation differs from the one encountered in the weak paramagnet $UGe_3$ in which a positive induced magnetization distribution at the Ge site has been found.[36]

## ACKNOWLEDGMENTS

We would like to warmly thank R. Ballou, J. Pécaut, G. Venturini, and C. Wilkinson for fruitful discussions, and for the kind help they provided us.

*Also at University Joseph Fourier, Grenoble, France
[1] E.S. Makarov and V.N. Bykov, Sov. Phys. Crystallogr. **4**, 164 (1959).
[2] C.E. Olsen, J. Appl. Phys. **31**, 340S (1960).
[3] A. Menovsky, F. R. de Boer, P. H. Frings, and J. J. M. Franse, in *High Field Magnetism*, edited by M. Date (North-Holland, Amsterdam, 1983), p. 189.
[4] Y. Onuki, S.W. Yun, I. Ukon, I. Umehara, K. Satoh, I. Sakamoto, M. Hunt, P. Meeson, P. Probst, and M. Springford, J. Phys. Soc. Jpn. **60**, 2127 (1991).
[5] Y. Onuki, I. Ukon, S.W. Yun, I. Umehara, K. Satoh, T. Fukuhara, H. Sato, S. Takayanagi, M. Shikama, and A. Ochiai, J. Phys. Soc. Jpn. **61**, 293 (1992).
[6] S.W. Yun, K. Satoh, Y. Fujimaki, I. Umehara, Y. Ōnuki, S. Takayanagi, H. Aoki, S. Uji, and T. Shimizu, Physica B **186-188**, 129 (1993).
[7] G. Oomi, K. Nishimura, Y. Ōnuki, and S.W. Yun, Physica B **186-188**, 758 (1993).
[8] H. Takahashi, N. Mōri, Y. Ōnuki, and S.W. Yun, Physica B **186-188**, 772 (1993).
[9] G. Oomi, T. Kagayama, K. Nishimura, S.W. Yun, and Y. Ōnuki, Physica B **206-207**, 515 (1995).
[10] H. Yamagami and A. Hasegawa, Physica B **186-188**, 182 (1993).
[11] Y. Onuki, Physica B **186-188**, 92 (1993).
[12] K. Nishimura, G. Oomi, S.W. Yun, and Y. Ōnuki, J. Alloy Compnd. **213-214**, 383 (1994).
[13] K. Oikawa, T. Kamiyama, H. Asano, Y. Ōnuki, and M. Kohgi, J. Phys. Soc. Jpn. **65**, 3229 (1996).
[14] P. Boulet, A. Daoudi, M. Potel, H. Nöel, G.M. Gross, G. André, and F. Bourée, J. Alloy Compnd. **247**, 104 (1997).
[15] S.S. Saxena, P. Agarwal, K. Ahilan, F.M. Grosche, R.K.W. Haselwimmer, M.J. Steiner, E. Pugh, I.R. Walker, S.R. Julian, P. Monthoux, G.G. Lonzarich, A. Huxley, I. Sheikin, D. Braithwaite, and J. Flouquet, Nature (London) **406**, 587 (2000).
[16] A. Huxley, I. Sheikin, E. Ressouche, N. Kernavanois, D. Braithwaite, R. Calemczuk, and J. Flouquet, Phys. Rev. B **63**, 144519 (2001).
[17] D. Fay and J. Appel, Phys. Rev. B **22**, 3173 (2000).
[18] R. Roussev and A.J. Millis, Phys. Rev. B **63**, 140504 (2001).
[19] A.B. Shick and W.E. Pickett, Phys. Rev. Lett. **86**, 300 (2001).

[20] H. Yamagami (unpublished).
[21] P. Wolfers, J. Appl. Crystallogr. **23**, 554 (1990).
[22] $R_\omega(F^2)=\sqrt{\Sigma[(I_{\rm obs}-I_{\rm calc})/\sigma_{I_{\rm obs}}]^2/\Sigma[I_{\rm obs}/\sigma_{I_{\rm obs}}]^2}$ where $I_{\rm obs}$ and $I_{\rm calc}$ are the observed and calculated intensities, respectively, and $\sigma_{I_{\rm obs}}$ is the standard deviation.
[23] P.J. Becker and P. Coppens, Acta Crystallogr., Sect. A: Cryst. Phys., Diffr., Theor. Gen. Crystallogr. **30**, 129 (1974).
[24] J.C. Le Guillou and J. Zinn-Justin, J. Phys. (France) Lett. **46**, L137 (1985).
[25] R. Nathans, M.T. Pigott, and C.G. Shull, J. Phys. Chem. Solids **6**, 38 (1958).
[26] S.F. Gull and G.J. Daniell, Nature (London) **272**, 686 (1978).
[27] J. Skilling and S.F. Gull, in *Maximum Entropy and Bayesian Methods in Inverse Problems*, edited by C. Ray Smith and W.T. Grandy, Jr. (Reidel, Dordrecht, 1985), p. 83.
[28] R.J. Papoular and B. Gillon, Europhys. Lett. **13**, 429 (1990).
[29] A. Zheludev, R.J. Papoular, E. Ressouche, and J. Schweizer, Acta Crystallogr., Sect. A: Found. Crystallogr. **A51**, 450 (1995).
[30] P.J. Brown, J. Neutron Res. **4**, 25 (1996).
[31] E. Balcar and S.W. Lovesey, in *Theory of Magnetic Neutron and Photon Scattering* (Oxford Science Publications, Oxford, 1989), p. 28.
[32] P.J. Brown, in *International Tables for Crystallography* C, edited by A.J.C. Wilson (Kluwer Academic Publishers, Dordrecht, 1992), p. 391.
[33] J.P. Desclaux (unpublished).
[34] G. van der Laan and B.T. Thole, Phys. Rev. B **53**, 14 458 (1996).
[35] G.H. Lander, M.S.S. Brooks, B. Lebech, P.J. Brown, O. Vogt, and K. Mattenberger, J. Appl. Phys. **69**, 4803 (1991).
[36] G.H. Lander, J.F. Reddy, A. Delapalme, and P.J. Brown, Phys. Rev. Lett. **44**, 603 (1980).